Energy Materials

Supplementary Materials

Understanding Mg-ion deposition behavior on MgBi alloy in solid-state form

Qian Wang[1,2], Hao Li[3], Ting Xu[1], Yungui Chen[1,4], Yigang Yan[1,4,*]

[1]Institute of New Energy and Low-Carbon Technology, Sichuan University, Chengdu 610065, Sichuan, China.

[2]College of Materials Science and Engineering, Sichuan University, Chengdu 610065, Sichuan, China.

[3]Advanced Institute for Materials Research (AIMR), Tohoku University, Sendai 980-8577, Japan.

[4]Engineering Research Center of Alternative Energy Materials and Devices, Ministry of Education, Sichuan University, Chengdu 610065, Sichuan, China.

[*]**Correspondence to:** Prof./Dr. Yigang Yan, Institute of New Energy and Low-Carbon Technology, Sichuan University, Chengdu 610065, Sichuan, China. E-mail: yigang.yan@scu.edu.cn

Table 1. Study on the solid-state electrolytes for Mg-ion batteries

Symmetric cell	Current density (mA cm^{-2})	T (°C)	Voltage (V)	Cycled time (h)	DOI
Mg | $Mg(BH_4)_2 \cdot CH_3NH_2$ | Mg	0.01	60	0.06	120	10.1021/acs.chemmater.2c03641
Mg | am-$Mg(BH_4)_2 \cdot 2NH_3$ | Mg	0.1	75	0.05	600	10.1002/eem2.12527
Mg | $Mg(BH_4)_2 \cdot 1.6NH_3$-MgO(60 wt.%) | Mg	0.25	60	0.07	52	10.1021/acsaem.0c01599
Mg | $Mg(BH_4)_2 \cdot 1.5NH_3$-	0.1	60	0.24	250	10.1016/j.ens

YSZ(60 wt.%) | Mg					m.2022.07.012
Mg | $Mg(BH_4)_2$·1.5THF-MgO(75 wt%) | Mg	0.1	55	0.26	100	10.1002/batt.202200163
Mg | MBN | Mg	0.1	50	1	116	10.1039/d3cc00994g
Mg | MBN-Br | Mg	0.1	50	0.03	416	10.1039/d3cc00994g
Mg20Bi | MBN | Mg20Bi	0.1	50	0.6	600	This work
Mg20Bi | MBN-Br | Mg20Bi	0.1	50	0.05	600	This work

Note. am-$Mg(BH_4)_2$·$2NH_3$: Amorphous $Mg(BH_4)_2$·$2NH_3$; YSZ: Y_2O_3-ZrO_2; MBN: $Mg(BH_4)_2$·$1.9NH_3$; MBN-Br: $Mg(BH_4)_2$·$1.9NH_3$-$MgBr_2$·$2NH_3$(32 wt.%).

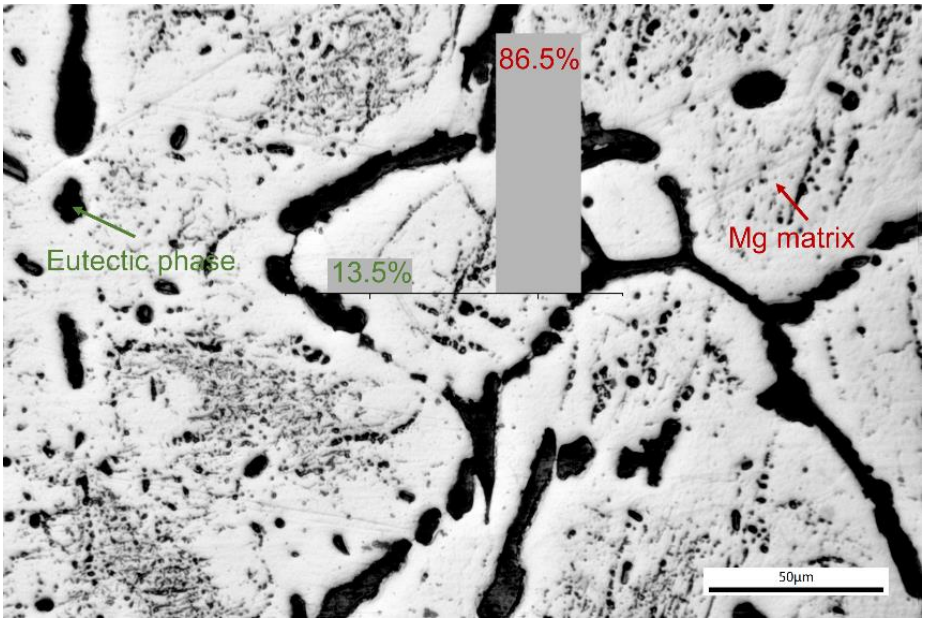

Figure 1. Optical Micrograph (black regions denote eutectic phases) of Mg20Bi alloy. Inset, the proportion of eutectic phase and Mg matrix. The content of the eutectic phase was calculated by Image Pro Plus 6.0.

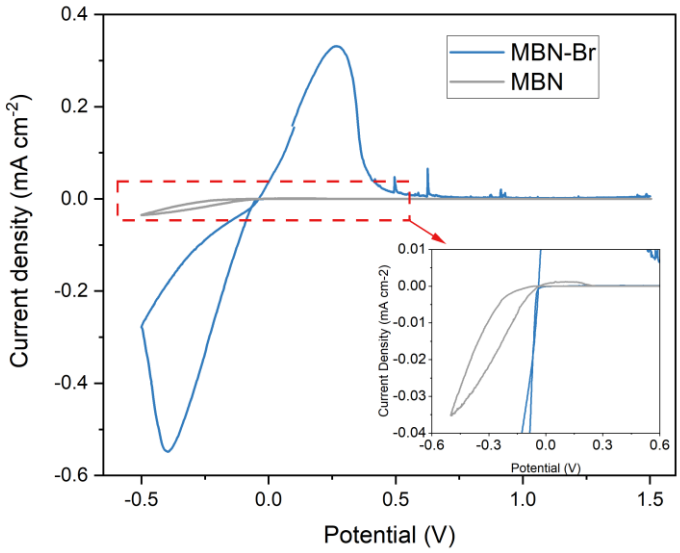

Figure 2. Cyclic voltammetry curves of Mg20Bi alloy anode with MBN and MBN-Br as electrolytes, respectively.

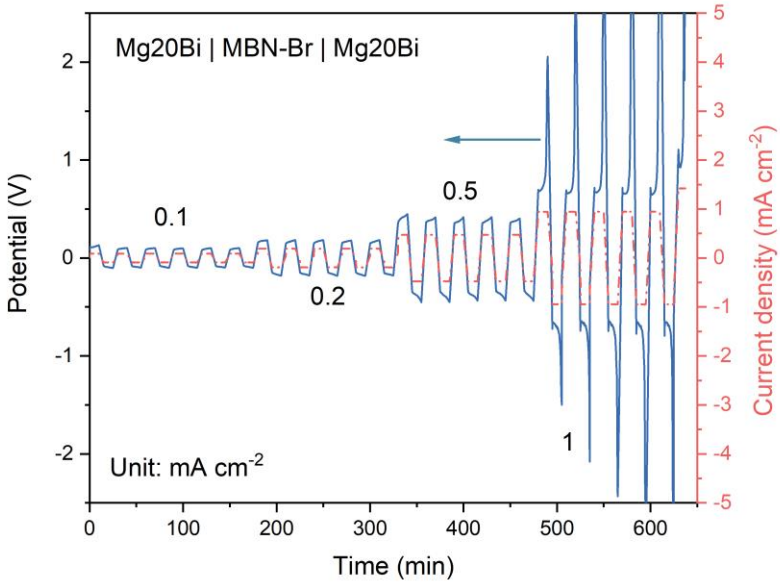

Figure 3. Galvanostatic cycling of the symmetric cell at different current densities of 0.1 to 1 mA cm^{-2}.

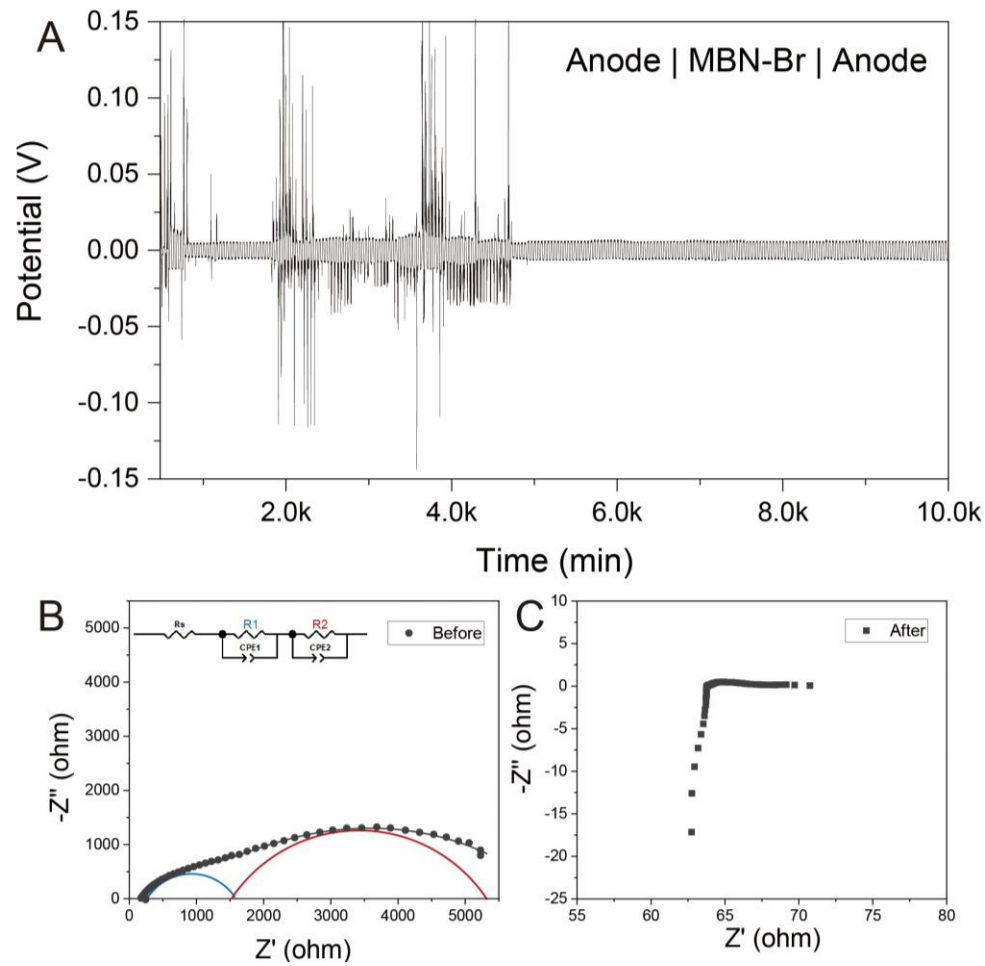

Figure 4. Electrochemical performance of anode with MBN-Br. (A) Long-term cycling curve at 0.1 mA cm^{-2}; Nyquist plots of the Anode | SSEs | Anode symmetric cell before and after Mg stripping/plating: (B) Before and (C) After.

As shown in Figure 4A, the overpotential of the symmetric cell exhibits a significant drop during the initial cycles, followed by gradual stabilization after multiple cycles. The response of overpotential to current ultimately resembles the performance of a normal cell. The impedance spectra of the initial symmetric cell [Figure 4B] reveal typical ionic conductor characteristics, i.e., the presence of multiple semicircles. However, the impedance spectra of the symmetric cell undergo significant changes with extended cycling [Figure 4C]. The high-frequency impedance values become negative, while the low-frequency impedance approaches zero, indicating inductive effects that may related to a short circuit[1].

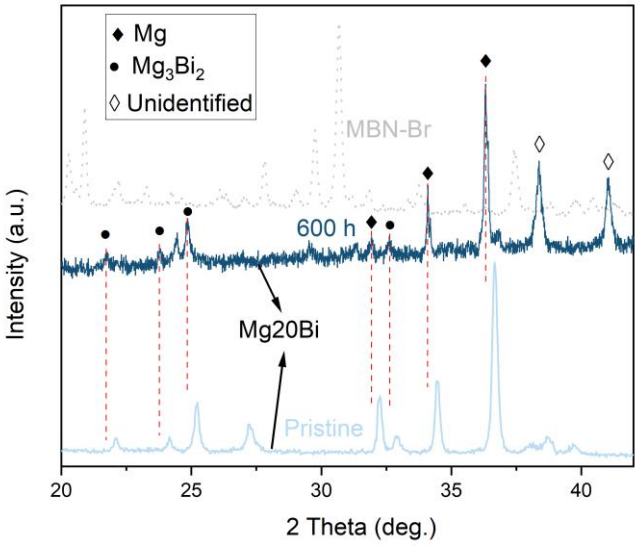

Figure 5. XRD patterns of alloy anode surface before and after Mg stripping/plating.

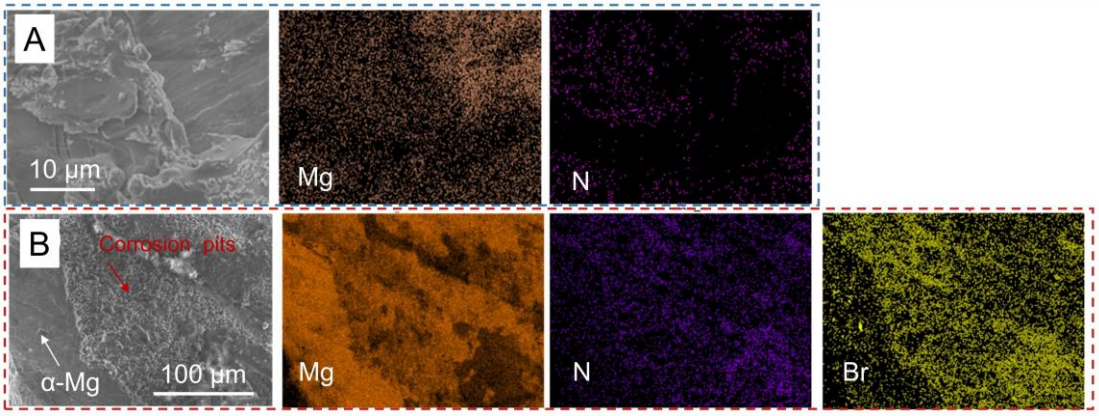

Figure 6. Mg anode after cycling in Mg | SSEs | Mg symmetric cell. SEM-EDS images of the Mg anode after long cycling with different SSEs: (A) MBN and (B) MBN-Br.

After long cycling of magnesium with MBN electrolyte, a laminar structure appeared on the surface (as shown in Figure 6A), which prevented the stabilization of the Mg ions for electroplating/stripping. Conversely, with the MBN-Br composite electrolyte, corrosion pits were observed on the surface of the magnesium anode after extended cycling, indicated by the red arrows in Figure 6B. Additionally, elemental Br

aggregation was detected in these areas, which we hypothesize is related to the etching effect of Br^- ions. Furthermore, since only the α-Mg matrix phase is present in the Mg anode (as indicated by the white arrow in Figure 6B), it is challenging to directly observe the formation of the passivation layer from the MBN electrolyte and the subsequent corrosion process initiated by Br^- ions in the MBN-Br electrolyte.

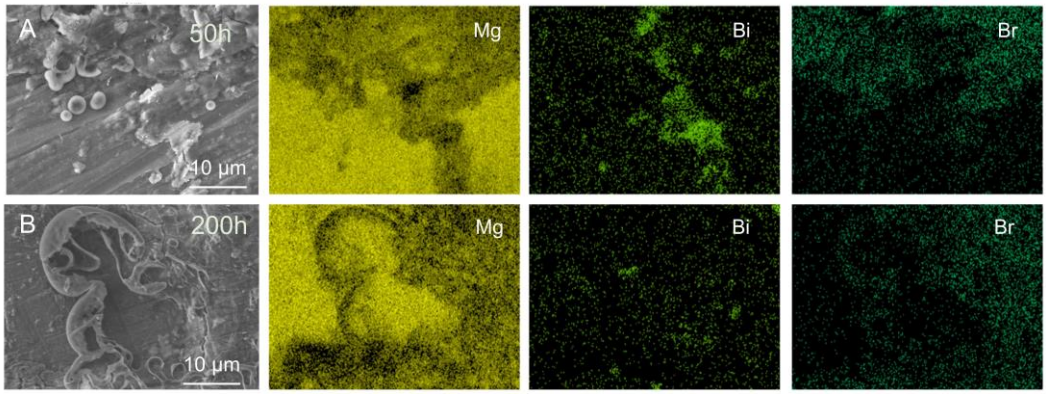

Figure 7. SEM images and EDS results of Mg20Bi alloy anode from the symmetric cell after different times of stripping/plating: (A) 50 h and (B) 200 h.

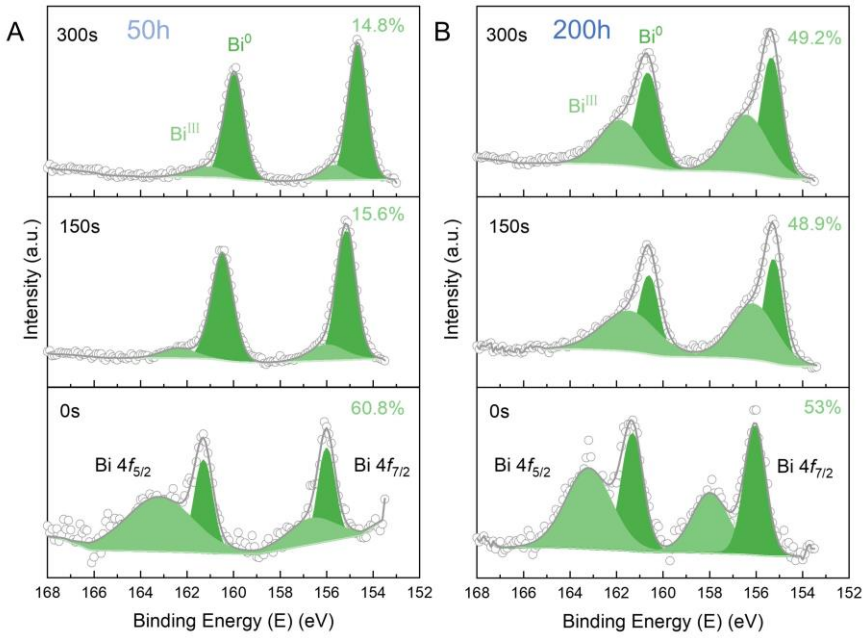

Figure 8. Bi 4*f* spectra of Mg20Bi alloy anode were etched for different etching times from the symmetric cell after different stripping/plating times: (A) 50 h and (B) 200 h. The binding energy of Bi 4*f* spectra of Mg20Bi alloy anode cycling after 50 h at 0 s is

higher than at 150 s and 300 s, e.g., 163.2 eV, 162.4 eV and 161.1 eV, same with the Bi^{III} binding energy for Bi $4f_{5/2}$, respectively. For the Mg20Bi alloy anode cycling after 200 h, the Bi^{III} binding energy for Bi $4f_{5/2}$ changed from 163.3 eV at 0 s to 161.6 eV at 150 s and 161.8 eV at 300 s.

REFERENCES

1. Harrington DA, van den Driessche P. Mechanism and equivalent circuits in electrochemical impedance spectroscopy. *Electrochimica Acta* 2011;56:8005-13. DOI: 10.1016/j.electacta.2011.01.067.